Pathology - Research and Practice 215 (2019) 712–721

Contents lists available at ScienceDirect

Pathology - Research and Practice

journal homepage: www.elsevier.com/locate/prp

Silencing of lncRNA MALAT1 inhibits cell cycle progression via androgen receptor signaling in prostate cancer cells

Xiaofan Dai[a], Lingyun Liu[a], Zuowen Liang[b], Kaimin Guo[a], Shengqi Xu[a], Hongliang Wang[a,*]

[a] Department of Andrology, The First Hospital of Jilin University, Changchun, 130021, People's Republic of China
[b] Human Sperm Bank of Jilin Province, The First Hospital of Jilin University, Changchun, 130021, People's Republic of China

ARTICLE INFO

Keywords:
Metastasis associated lung adenocarcinoma transcript 1
Prostate cancer
Androgen receptor
Long noncoding RNA
microRNA

ABSTRACT

Prostate cancer is the second common cancer in men with high morbidity and mortality. Androgen receptor (AR) signaling plays a crucial role in occurrence and development of prostate cancer. In this study, we demonstrated that lncRNA metastasis associated lung adenocarcinoma transcript 1 (MALAT1) was increased in prostate cancer cells after androgen stimulation, as well as AR. The silencing of MALAT1 inhibited dihydrotestosterone (DHT) administration-induced acceleration of proliferation and cell cycle progression, and increase of AR expression in prostate cancer cells. MALAT1 bound to miR-320b and negatively regulated its expression, and vice versa. AR is a target of miR-320b. The phenotypic changes induced by silencing of MALAT1 were abolished by miR-320b inhibition or AR overexpression. Additionally, MALAT1 knockdown also suppressed the tumorigenesis of prostate cancer cells in nude mice. In summary, the silencing of MALAT1 inactivated AR signaling by sponging miR-320b, and inhibited proliferation and cell cycle progression in prostate cancer cells, suggesting that MALAT1 may be a new target in diagnosis and therapy of prostate cancer in clinic.

1. Introduction

Prostate cancer is the second frequently diagnosed cancer in men, only less than lung cancer [1]. An estimated 1,111,700 new cases and 307,500 deaths of prostate cancer occurred in 2012 worldwide [1]. The pathogenesis of prostate cancer has not been elucidated, but it has been known that androgen and androgen receptor (AR) play crucial roles in prostate cancer progression [2]. Currently the most commonly used treatment for prostate cancer in clinic is androgen deprivation therapy (ADT, surgical or medical castration), which aims to block the AR signaling [3]. However, most patients relapse within several years, and the disease is generally more aggressive and is currently referred to as castration-resistant prostate cancer (CRPC) [3]. Several hypotheses were proposed to explain the CRPC, but none has been widely accepted. Therefore, it is significant to exploring possible new therapeutic targets in prostate cancer.

Over the years, the function of protein coding genes has been mainly focused in the prostate cancer progression. Although noncoding genes are much more than encoding genes, the conceptual and technical limitations restricted our knowledge of noncoding RNAs (ncRNAs) functions [4]. Recently, with the development of biological technologies, the ncRNAs attract an increasing attention [5]. ncRNAs are consist of short ncRNAs (< 200bp) and long ncRNAs (lncRNAs, > 200bp) [6]. LncRNAs regulate various cellular processes, including proliferation, differentiation, motility, development and diseases [7–9]. Lots of studies reported that lncRNAs play a crucial role in prostate cancer progression. In 1999, lncRNA prostate cancer antigen 3 (PCA3) was found highly expressed in prostate cancer tissues, and identified as the first prostate cancer-specific lncRNA [10]. Prostate cancer associated ncRNA transcript-1 (PCAT-1) is upregulated in prostate cancer, and promotes proliferation, invasion and metastasis through c-myc [11]. Metastasis associated lung adenocarcinoma transcript1 (MALAT1) has been reported to be highly expressed in prostate cancer specimens, and silencing of MALAT1 inhibits proliferation, migration and invasion in prostate cancer cells [12]. MALAT1 in highly expressed in enzalutamide-resistant prostate cancer cells (enzalutamide is an AR antagonist) [13], suggesting that the function of MALAT1 may be associated with AR. AR signaling is essential for prostate development and prostate cancer progression, and the low dose of androgen administration enhances proliferation of prostate cancer cells [14]. However, the relationship between MALAT1 and AR remains unclear. In this study, we studied the effect of MALAT1 on AR-positive prostate cancer cells, attempted to investigate whether its role is associated with AR signaling.

* Corresponding author at: Department of Andrology, The First Hospital of Jilin University, 71 Xinmin Avenue, Changchun, 130021, People's Republic of China.
E-mail address: whongliang2015@163.com (H. Wang).

https://doi.org/10.1016/j.prp.2019.01.011
Received 19 October 2018; Received in revised form 18 December 2018; Accepted 5 January 2019
0344-0338/

Table 1
The sequence information of real-time PCR primers, knockdown primers and amplification PCR primers used in this study.

Name	Sequence (5'-3')
MALAT1 forward	5'-GACTTCAGGTCTGTCTGTTCT-3'
MALAT1 reverse	5'-CAACAATCACTACTCCAAGC-3'
GAPDH forward	5'-GAAGGTCGGAGTCAACGGAT-3'
GAPDH reverse	5'-CCTGGAAGATGGTGATGGGAT-3'
shMALAT1 sense	5'-GATCCCCGGAAGATAGAAACAAGATATTCAAGAGATATCTTGTTTCTATCTTCCTTTTT-3'
shMALAT1 antisense	5'-AGCTAAAAAGGAAGATAGAAACAAGATAtctcttgaaTATCTTGTTTCTATCTTCCGGG-3'
shRNA NC sense	5'-GATCCCCTTCTCCGAACGTGTCACGTTTCAAGAGAACGTGACACGTTCGGAGAATTTTT-3'
shRNA NC antisense	5'-AGCTAAAAATTCTCCGAACGTGTCACGTTCTCTTGAAACGTGACACGTTCGGAGAAGGG-3'
miR-320b RT	5'-GTTGGCTCTGGTGCAGGGTCCGAGGTATTCGCACCAGAGCCAACTTGCCC-3'
U6 RT	5'-GTTGGCTCTGGTGCAGGGTCCGAGGTATTCGCACCAGAGCCAACAAAATATGG-3'
miR-320b forward	5'-GCCGCAAAAGCTGGGTTGA-3'
U6 forward	5'-GCTTCGGCAGCACATATACT-3'
miRNA reverse	5'-GTGCAGGGTCCGAGGTATTC-3'
AR amplification forward	5'-CACGGATCCATGATACTCTGGCTTCACAG-3'
AR amplification reverse	5'-CACCTCGAGTCACTGGGTGTGGAAATAGAT-3'

Abbreviation: MALAT1metastasis-associated lung ademocarcinoma transcript 1; GAPDHglyceraldehydes phosphate dehydrogenase; NCnegative control; ARandrogen receptor.

2. Material and methods

2.1. Plasmid construction

To construct the lncRNA MALAT1 knockdown plasmid, two strands containing a sequence which targeted the 5′-GGAAGATAGAAACAAG ATA-3′ in MALAT1 transcript were synthesized. The two strands were annealed and inserted into pRNAH1.1 vector at *BamHI* and *HindIII* sites. The sequence information of the sense and antisense strands was shown in Table 1.

AR (NM_001011645.3) coding region (CDS) sequence was amplified with human cDNA, in presence of amplification PCR primers. After sequence analysis, the fragment was inserted into pcDNA3.1 vector with *BamHI* and *Xhol* sites. The sequence information of the AR CDS amplification PCR primers was shown in Table 1.

2.2. Cell culture, transfection and drug treatment

Human prostate cancer cell lines DU145 was purchased from Procell (Wuhan, Hubei, China), and cultured with MEM medium (Procell) supplemented with 10% fetal bovine serum (FBS) (Hyclone, Logan, UT, USA) at 37 ℃ in 5% CO_2. Human prostate cancer cell line PC3 was purchased from Procell and cultured with Ham's F-12 K medium (Procell). Human prostate cancer cell lines LNCaP and 22Rv1 were purchased from Zhongqiaoxinzhou (Shanghai, China) and cultured in RPMI-1640 medium (Gibco BRL, Gaithersburg, MD, USA) supplemented with 10% FBS at 37 ℃ in 5% CO_2. The LNCaP and 22Rv1 cells were transfected with plasmids containing MALAT1 shRNA or NC sequence in serum-free medium using lipofectamine reagent (Invitrogen, Carlsbad, CA, USA). At 24 h post-transfection, the cells were treated with 100 μg/ml G418 (Invitrogen), and the medium was refreshed every 2–3 days. About one week later, the single cells were selected and cultured in G418-free medium for about 2 weeks. The MALAT1 stably knocked down cell lines were obtained.

When the confluence reached 70%, the LNCaP or 22Rv1 cells were treated with 50 nM dihydrotestosterone (DHT) (MCE, NJ, USA) for different times [15]. The cells in control groups were treated with the solvent of DHT.

2.3. RNA extract, reverse transcription and real-time PCR

The total RNA was extracted with a TRIpure RNA extraction kit (BioTeke, Beijing, China). After concentration mearsurement, the RNA was reversely transcribed into cDNA with M-MLV reverse transcriptase (BioTeke) in the presence of Oligo(dT) and random primers, or specific miRNA RT primers (Sangon, Shanghai, China).

The cDNA was used for real-time PCR with 2xPower Taq PCR Master Mix (BioTeke) and SYBR Green (Solarbio, Beijing, China), to detect the RNA level of MALAT1 and miR-320b, with GAPDH or U6 as the internal control. The PCR procedure was set as follow: 94 ℃ for 5 min, 94 ℃ for 10 s, 60 ℃ for 20 s, 72 ℃ for 30 s, followed with 40 cycles of 72 ℃ for 2 min 30 s, 40 ℃ for 1 min 30 s, melting from 60 ℃ to 94 ℃ each 1 ℃ for 1 s, and finally incubated at 25 ℃ for several minutes. The PCR data were analyzed with $2^{-\Delta\Delta Ct}$ method. The sequence information of real-time PCR primers was shown in Table 1.

2.4. CCK-8 assay

CCK-8 assay was performed to detect the viability of LNCaP or 22Rv1 cells. The cells were seeded in 96-well plates at a density of 4×10^3 per well. After culturing for 24 h, 48 h or 72 h, the cells were incubated with CCK-8 reagent (Beyotime, Haimen, Jiangsu, China) of 10 μl per well for 1 h. After incubation, the optical density of the medium was measured by microplate reader at 450 nm.

2.5. Flow cytometry

Flow cytometry was performed to detect the cell cycle phases of LNCaP and 22Rv1 cells. After culturing to a confluence of 90%, the cells were collected and washed with PBS. Then the cells were fixed in precooling 70% ethanol at 4 ℃ for 2 h, treated with the cell cycle analysis kit (Beyotime) according to the manufacturer's protocols, and detected with a flow cytometer (BD, Franklin Lakers, NJ, USA).

2.6. Western blot

The total cellular protein was extracted from cells by RIPA lysis buffer (Beyotime), and the concentration was measured by BCA protein quantification kit (Beyotime). After denaturation by boiling, the protein was separated by SDS-PAGE, and transferred onto PVDF membrane (Millipore, Boston, MA, USA). After blocking with 5% skim milk for 1 h at room temperature, the PVDF membrane was incubated with one of the following antibodies at 4 ℃ overnight: rabbit anti-AR (1:500; Proteintech), mouse anti-cyclin D1 (1:500; Proteintech; Wuhan, Hubei, China), rabbit anti-cyclin-dependent kinase 6 (CDK6) (1:500; Proteintech), rabbit anti-p27 (1:500; Proteintech), rabbit anti-GAPDH (1:500; Bioss, Beijing, China). After rinsing with PBS, the membrane was incubated with goat anti-mouse or anti-rabbit secondary antibody at 37 ℃ for 45 min, reacted with ECL reagent (Beyotime), and followed with a signal exposure. The bands were analyzed with Gel-Pro-Analyzer software, with GAPDH as the internal control.

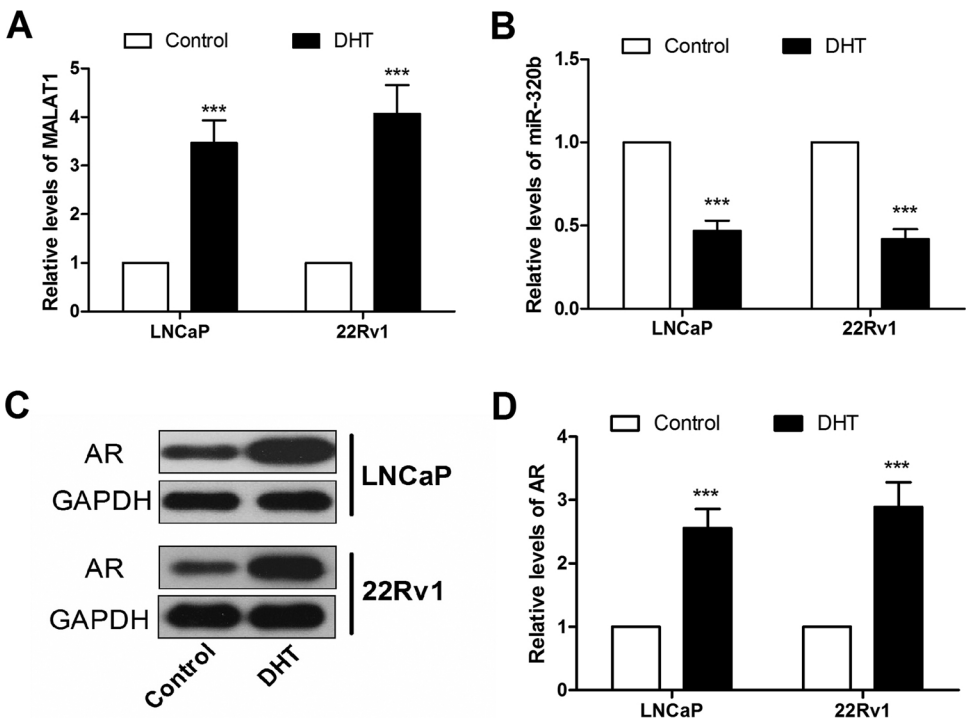

Fig. 1. lncRNA MALAT1 was increased in prostate cancer cells after DHT stimulation. (A) The lncRNA MALAT1 levels in LNCaP or 22Rv1 cells with DHT administration were detected by real-time PCR. (B) The miR-320b levels in LNCaP or 22Rv1 cells without DHT administration. (C–D) The AR mRNA levels in LNCaP or 22Rv1 cells after DHT treatment detected by western blot. (n = 3) (*$P < 0.05$, **$P < 0.01$, ***$P < 0.001$, *ns, no significance*; lncRNA, long noncoding RNA, MALAT1, metastasis associated lung adenocarcinoma transcript 1, DHT, dihydrotestosterone, GAPDH, glyceraldehydes phosphate dehydrogenase).

2.7. Luciferase reporter assay

The luciferase reporter assay was performed to verify the binding relation of miR-320b and MALAT1. The sequence targeted MALAT1 or mutant sequence was cloned into luciferase reporter vector pmirGLO with *NheI* and *SalI* sites. The 293 T cells were transfected with the luciferase reporter vector and miR-320b mimics. After culturing for 48 h, the cells were treated with luciferase reporter assay system (Promega, Madison, WI, USA), and the Firefly and Renilla values were measured with a microplate reader (TECAN, Zurich, Swizerland).

2.8. Tumorigenesis assay in vivo

The animals in this study were taken care of and sacrificed according to Guide for the Care and Use of Laboratory Animals (8^{th} edition, NIH). The experiment procedures were approved by the Ethics Committee of Jilin University.

Healthy 8-week old BALB/cA-nu mice (HFK, Beijing, China) were kept in a controlled environment (22 ± 1 ℃ and a humidity of 45–55% with a 12 h/12 h light/dark cycle) with free access to food and water. After acclimatization to the environment for one week, the mice were randomly divided into 4 groups: LNCaP NC, LNCaP shMALAT1, 22Rv1 NC and 22Rv1 shMALAT1 (n = 6). The mice in LNCaP NC and LNCaP shMALAT1 groups were subcutaneously injected with 0.1 ml cell suspension containing 1×10^7 LNCaP cells stably expressing NC or MALAT1 shRNA. The mice in 22Rv1 NC and 22Rv1 shMALAT1 groups were subcutaneously injected with 0.1 ml cell suspension containing 1×10^7 22Rv1 cells stably expressing NC or MALAT1 shRNA. After inoculation of LNCaP or 22Rv1 cells one week, the subcutaneous nodules could be observed by naked eyes. The size of nodules was measured with a vernier caliper at day 7, 10, 13, 16, 19 and 21 post-inoculation. After the last measurement, the mice were anaesthetized and sacrificed, and the subcutaneous nodules were collected for detections.

2.9. Immunohistochemical assay

The nodule tissues were fixed with formaldehyde overnight, and washed with flow water. Then the tissues were dehydrated with ethanol of grading concentrations (70% for 2 h, 80% overnight, 90% for 2 h, 100% for 1 h twice), hyalinized with xylene, and embedded in paraffin. The paraffin block was cut into section of 5 μm, and dried at 60 ℃. The sections were dewaxed with xylene ethanol. Subsequently, the sections were treated with boiling antigen repair buffer for 10 min. After blocking with H_2O_2 (Sinopharm, Beijing, China) for 15 min and goat serum for 15 min, the sections were incubated with rabbit antibody against prostate specific antigen (PSA) (1:50; Proteintech) at 4 ℃ overnight. After washing with PBS, the sections were incubated with goat anti-rabbit biotin-conjugated IgG (1:200; Beyotime) at 37 ℃ for 30 min, incubated with HRP-labeled streptavidin (1:200; Beyotime) at 37 ℃ for 30 min, and reacted with DAB reagent (Solarbio). Finally, the sections were stained with hematoxylin (Solarbio) for 3 min, dehydrated with ethanol, hyalinized with xylene, mounted with gum, and photographed at 400x magnification.

2.10. Immunofluorescence assay

The nodule tissues were made into paraffin sections as previously described. The sections were dewaxed with xylene and ethanol, and reacted with boiling antigen repair buffer. After blocking with goat serum for 15 min, the sections were incubated with both rabbit antibody against AR (1:50; Proteintech) at 4 ℃ overnight. After washing with PBS, the sections were incubated with goat anti-rabbit IgG labeled with FITC (1:200; Beyotime) at room temperature for 90 min. Finally, the sections were counterstained with DAPI, mounted with antifading medium (Solarbio), and observed with a fluorescence microscope (Olympus, Tokyo, Japan) at 400x magnification.

2.11. Statistical analysis

The data in this study were presented as mean ± SD with three (*in vitro*) or six (*in vivo*) individuals, and analyzed with one-way or two-way ANOVA test with post hoc Bonferroni's multiple comparisons. A p value was seen as statistically significant when it was less than 0.05. (*P < 0.05, **P < 0.01, ***P < 0.001, ns, no significance)

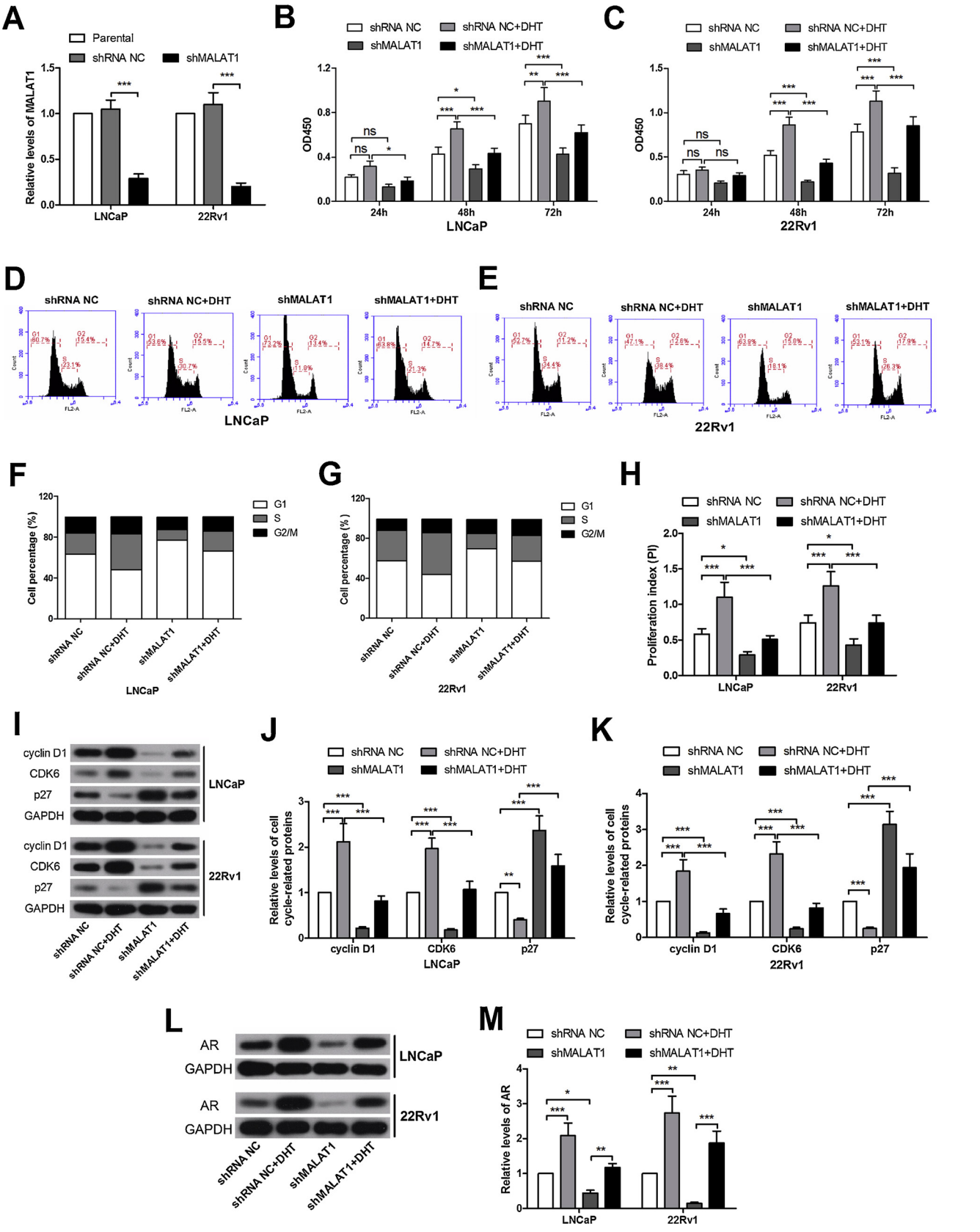

(caption on next page)

Fig. 2. Silencing of MALAT1 delayed cell cycle progression in prostate cancer cells.
(A) Real-time PCR was performed to measure the expression levels of MALAT1 after knockdown. (B–C) The CCK-8 assay was performed to detect the viability of LNCaP or 22Rv1 cells with or without DHT stimulation. (D–E) The flow cytometry images of LNCaP and 22Rv1 cells with or without DHT treatment. (F–G) The percentage of LNCaP or 22Rv1 cells in each cell cycle phase. (H–I) The proliferation index (PI) of LNCaP and 22Rv1 cells (PI = (S + G2/M)/G1). (J–K) The levels of cyclin D1, CDK8 and p27 in LNCaP and 22Rv1 cells with or without DHT administration were detected by western blot. (L–M) Western blot was performed to determine the AR expression levels in LNCaP and 22Rv1 cells with DHT treatment or/and MALAT1 knockdown. (n = 3) (*$P < 0.05$, **$P < 0.01$, ***$P < 0.001$, *ns, no significance*; MALAT1, metastasis associated lung adenocarcinoma transcript 1, DHT, dihydrotestosterone, CDK6, cyclin-dependent kinase 6, GAPDH, glyceraldehydes phosphate dehydrogenase, AR, androgen receptor).

3. Results

3.1. LncRNA MALAT1 was increased in prostate cancer cells after DHT stimulation

The two androgen-sensitive prostate cancer cell lines, LNCaP and 22Rv1, were treated with 50 nM DHT for 24 h, and the MALAT1 expression levels were found to be increased 3.47-fold and 4.07-fold, respectively, compared to the solvent-treated cells (Fig. 1A). Then the expression levels of miR-320b and AR were determined. The results showed that the expression levels of miR-320b decreased by more than 50% (Fig. 1B), while that of AR elevated 2.56-fold and 2.89-fold in LNCaP and 22Rv1 cells, respectively, after DHT administration (Fig. 1C–D). We also detected the expression levels of MALAT1 in AR negative prostate cancer cell lines DU145 and PC3 after DHT treatment. The results presented that the AR stimulation induced the increase of MALAT1 in DU145 and PC3 cells, which was not as significant as that in LNCaP and 22Rv1 cells (Fig. S1). These results suggested that the expression of AR was associated with MALAT1 and miR-320b under DHT administration, and there may be negative relationship between MALAT1 and miR-320b.

3.2. Silencing of MALAT1 delayed cell cycle progression in prostate cancer cells with or without androgen stimulation

To investigate the role of MALAT1 in prostate cancer cells, LNCaP or 22Rv1 cells were transfected with a shRNA targeting MALAT1 sequence to silence MALAT1 expression, and the inhibition effectiveness of the silencing was verified by real-time PCR (Fig. 2A). The CCK-8 assay results showed that the silencing of MALAT1 inhibited the cell viability whether with DHT treatment or not (Fig. 2B–C). The cell cycle transition from G1 to S phase in LNCaP and 22Rv1 cells was delayed by MALAT1 knockdown with or without DHT stimulation (Fig. 2D–G). The proliferation index (PI) was also showed a decline in MALAT1-silenced cells (Fig. 2H). Subsequently, the expression levels of several cell cycle-related proteins were detected. The cell cycle-dependent proteins cyclin D1 and CDK6 levels were decreased, and cell cycle inhibitor p27 level was increased dramatically in MALAT1-silenced cells whether with DHT application or not (Fig. 2I–K). In addition, the DHT-induced increase of AR expression level was attenuated after MALAT1 knockdown (Fig. 2L–M), suggested that MALAT1 played its roles via AR signaling in prostate cancer cells.

3.3. MALAT1 regulated AR expression by sponging miR-320b

The bioinformatic website StarBase 2.0 (http://starbase.sysu.edu.cn/browseNcRNA.php) was used to predict the candidate miRNAs of MALAT1. We found that miR-320b bound to the position of 3994–4000 and 7353–7359 of MALAT1 (Fig. 3A), and the binding was examined by luciferase reporter assay. As shown in Fig. 3B, miR-320b mimics significantly reduced the Firefly/Renilla values of the two MALAT1 sequences. The real-time PCR results revealed that the miR-320b levels were increased about 4-fold after MALAT1 knockdown (Fig. 3C). The expression levels of MALAT1 was decreased after miR-320b overexpression by transfection of mimics, and increased by miR-320b inhibitor (Fig. 3D), suggesting that MALAT1 may be a degradable sponge. A previous study reported that miR-320 family can target AR [16], and the binding relation was shown in Fig. 3E. The data from western blot showed that the expression level of AR was decreased by miR-320b mimics, and increased by miR-320b inhibitor significantly (Fig. 3E–F), which confirmed the regulation of miR-320b on AR in LNCaP and 22Rv1 cells.

3.4. Silencing of MALAT1-induced phenotypic changes were abolished by inhibition of miR-320b

To investigate the roles of MALAT1/miR-320b/AR axis, the MALAT1-silenced LNCaP and 22Rv1 cells were transfected with miR-320b inhibitor, and the phenotypes were detected. CCK-8 assay results revealed that the silencing of MALAT1-reduced cell viability was partly elevated by miR-320b inhibitor (Fig. 4A–B). The delays of cell cycle progression induced by MALAT1 knockdown were restored by inhibition of miR-320b (Fig. 4C–F). The shMALAT1-induced expression changes of cell cycle proteins, cyclin D1, CDK6 and p27 were also abolished by interference of miR-320b (Fig. 4G–I).

3.5. The phenotypic changes induced by MALAT1 knockdown was eliminated by AR expression

To further verify the roles of MALAT1/miR-320b/AR axis in prostate cancer, AR was overexpressed in MALAT1-knocked down LNCaP and 22Rv1 cells. The CCK-8 results showed that shMALAT1-induced viability changes in LNCaP and 22Rv1 cells were recovered by AR overexpression to some extent (Fig. 5A–B). The cell cycle arrest caused by silencing of MALAT1 was eliminated by ectopic expression of AR (Fig. 5C–F). AR also abolished the expression level changes of cell cycle-related proteins, cyclin D1, CKD6 and p27, initiated by MALAT1 knockdown (Fig. 5G–I). These results demonstrated that MALAT1 played its roles by sponging miR-320b from AR in prostate cancer cells.

3.6. MALAT1 knockdown inhibited tumorigenesis of prostate cancer cells in vivo

Subsequently, LNCaP or 22Rv1 cells were subcutaneously injected into nude mice, and cultured for 21 days. As shown in Fig. 5, the proliferation of LNCaP and 22Rv1 cells *in vivo* was inhibited significantly by MALAT1 knockdown from 7 days post-injection (Fig. 6A–C). At the 21st day, the weight of tumor formed by MALAT1-silenced LNCaP or 22Rv1 cells was lighter 44% or 70% than that of NC cells (Fig. 6D). Then immunohistochemical staining results showed that the PSA-positive cells in MALAT1-silenced tumors were decreased by 56% or 72%, compared with tumors formed by NC cells (Fig. 6E–F). The AR expression levels were decreased by more than 70 percent in the MALAT1-silenced tumors (Fig. 6G–H). Similar results were observed in the immunofluorescence assay (Fig. 6I–J). Above results suggested the antitumor effect of MALAT1 knockdown *in vivo*.

4. Discussion

LncRNA MALAT1 was first identified in non-small cell lung cancer (NSCLC) as a pro-tumor factor [17]. Subsequent studies reported its function in other tumors. MALAT1 is upregulated in liver cancer, breast

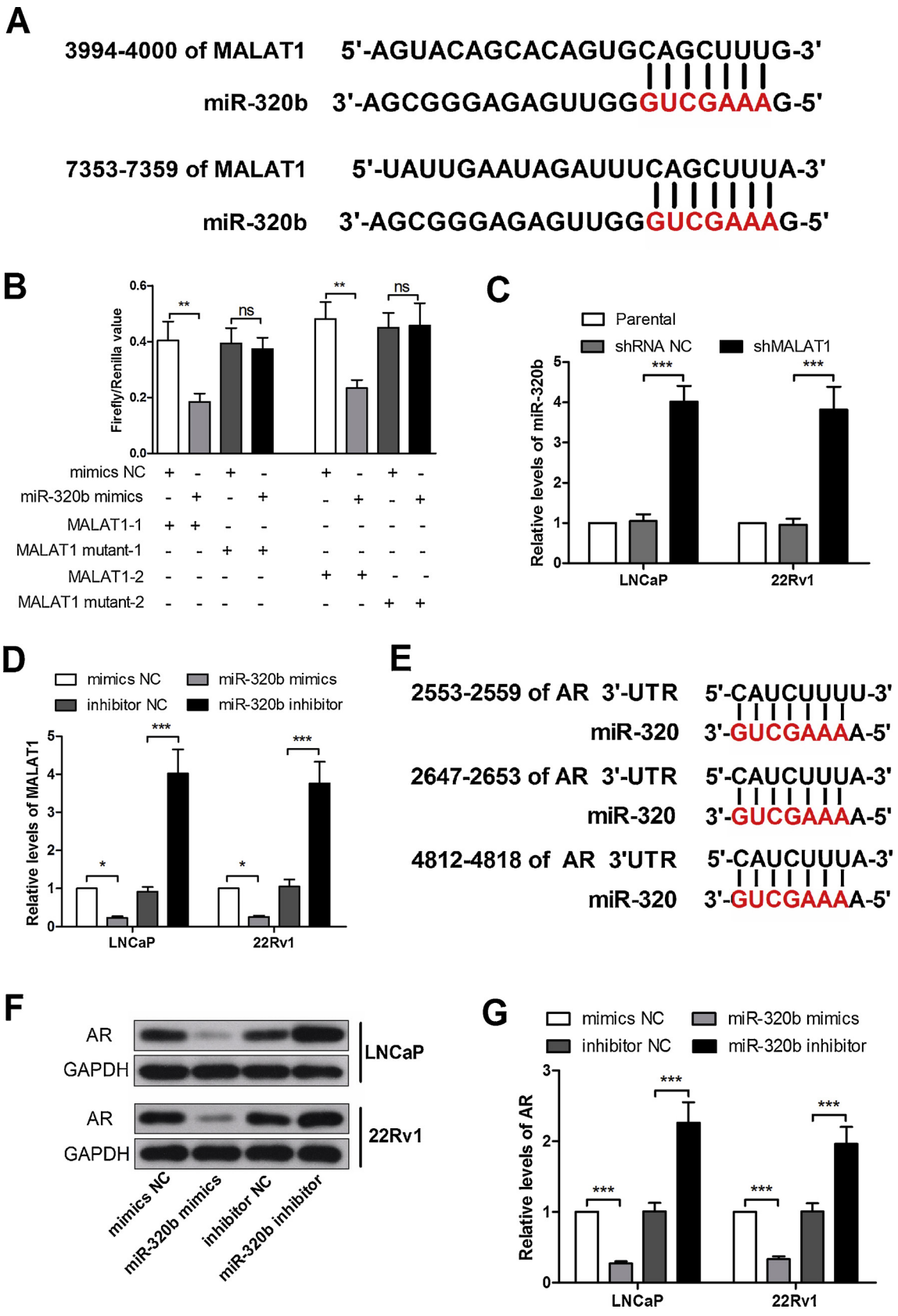

Fig. 3. MALAT1 knockdown suppressed AR expression level by sponging miR-320b.
(A) The seed sequence of miR-320b bound to two sequences of MALAT1. (B) The luciferase reporter assay was performed to verify the binding of miR-320b and MALAT1. (C) The level of miR-320b was detected by real-time PCR in MALAT1-silenced LNCaP and 22Rv1 cells. (D) The level of MALAT1 was detected after transfection of miR-320b mimics or inhibitor. (E) The seed sequence of miR-320 family members bound to AR 3′UTR. (F–G) The expression levels of AR were determined after miR-320b overexpression or inhibition. (n = 3) (*$P < 0.05$, **$P < 0.01$, ***$P < 0.001$, *ns, no significance*; MALAT1, metastasis associated lung adenocarcinoma transcript 1, DHT, dihydrotestosterone, AR, androgen receptor).

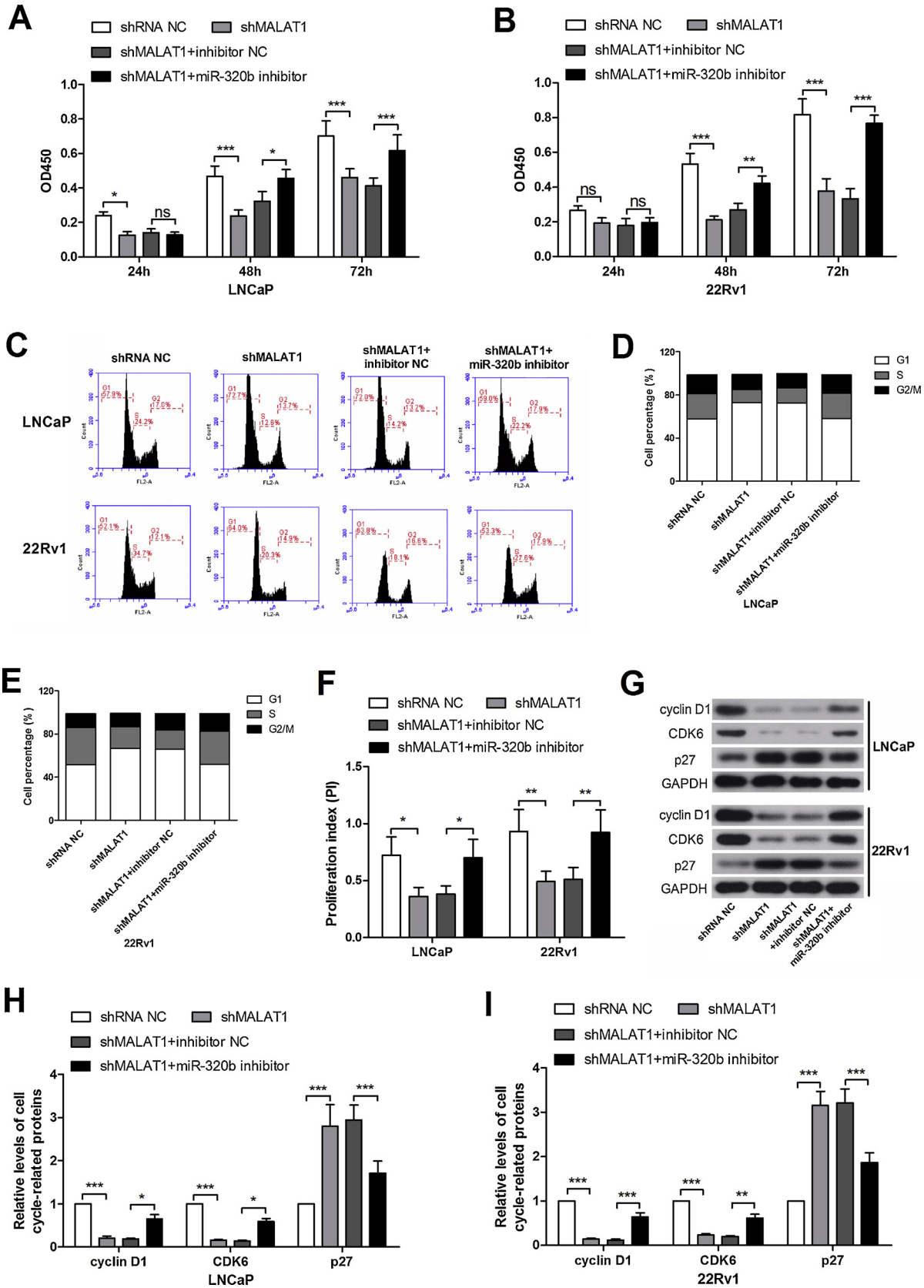

Fig. 4. Silencing of MALAT1-induced phenotypic changes were abolished by inhibition of miR-320b.
(A–B) CCK-8 assay was performed to detect the viability of LNCaP and 22Rv1 cells after inhibition of MALAT1 and miR-320b. (C) The images of flow cytometry detection of prostate cancer cells. (D–E) The percentage of LNCaP and 22Rv1 cells in each cell cycle phase. (F) The proliferation index (PI) of LNCaP and 22Rv1 cells was calculated as the percentage of cells in each phase (PI = (S + G2/M)/G1). (G–I) Western blot was performed to detect the expression levels of cell cycle-related proteins, cyclin D1, CDK6 and p27, with GAPDH as the internal control. (n = 3) (*$P < 0.05$, **$P < 0.01$, ***$P < 0.001$, *ns, no significance*; MALAT1, metastasis associated lung adenocarcinoma transcript 1, CDK6, cyclin-dependent kinase 6, GAPDH, glyceraldehydes phosphate dehydrogenase).

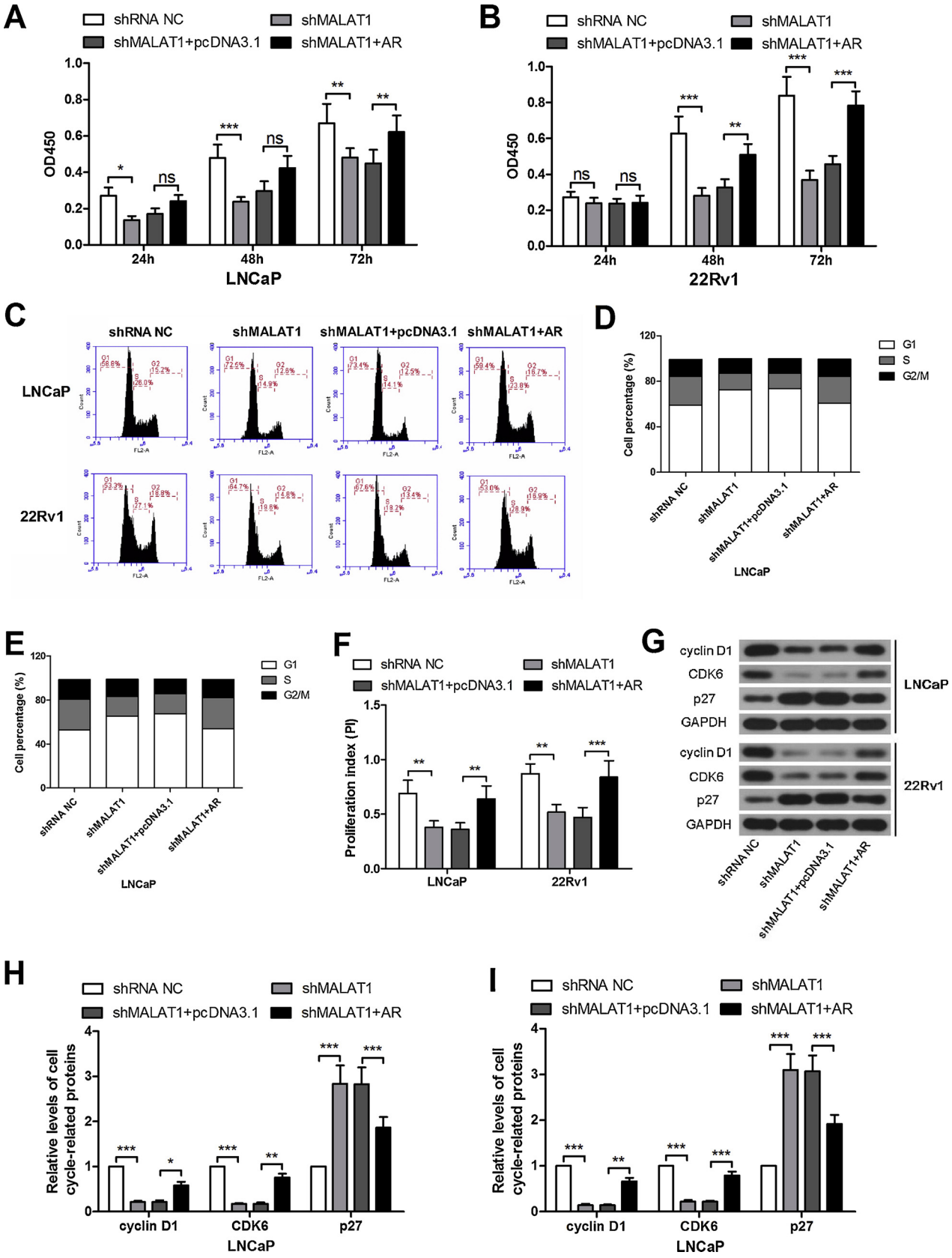

Fig. 5. The phenotypic changes induced by MALAT1 knockdown was eliminated by AR overexpression.
(A–B) The viability of LNCaP and 22Rv1 cells after MALAT1 knockdown and AR overexpression was detected by CCK-8 assay. (C) Flown cytometry was used for detection of cell cycle of LNCaP and 22Rv1 cells. (D–E) The cell percentage of LNCaP and 22Rv1 cells in each cell cycle phase. (F) The proliferation index (PI) was calculated according to the data in D and E (PI = (S + G2/M)/G1). (G–I) The expression levels of cyclin D1, CDK6 and p27 were determined by western blot after silencing of MALAT1 and ectopic expression of AR, with GAPDH as the internal control. (*$P < 0.05$, **$P < 0.01$, ***$P < 0.001$, *ns, no significance*; MALAT1, metastasis associated lung adenocarcinoma transcript 1, AR, androgen receptor, CDK6, cyclin-dependent kinase 6, GAPDH, glyceraldehydes phosphate dehydrogenase).

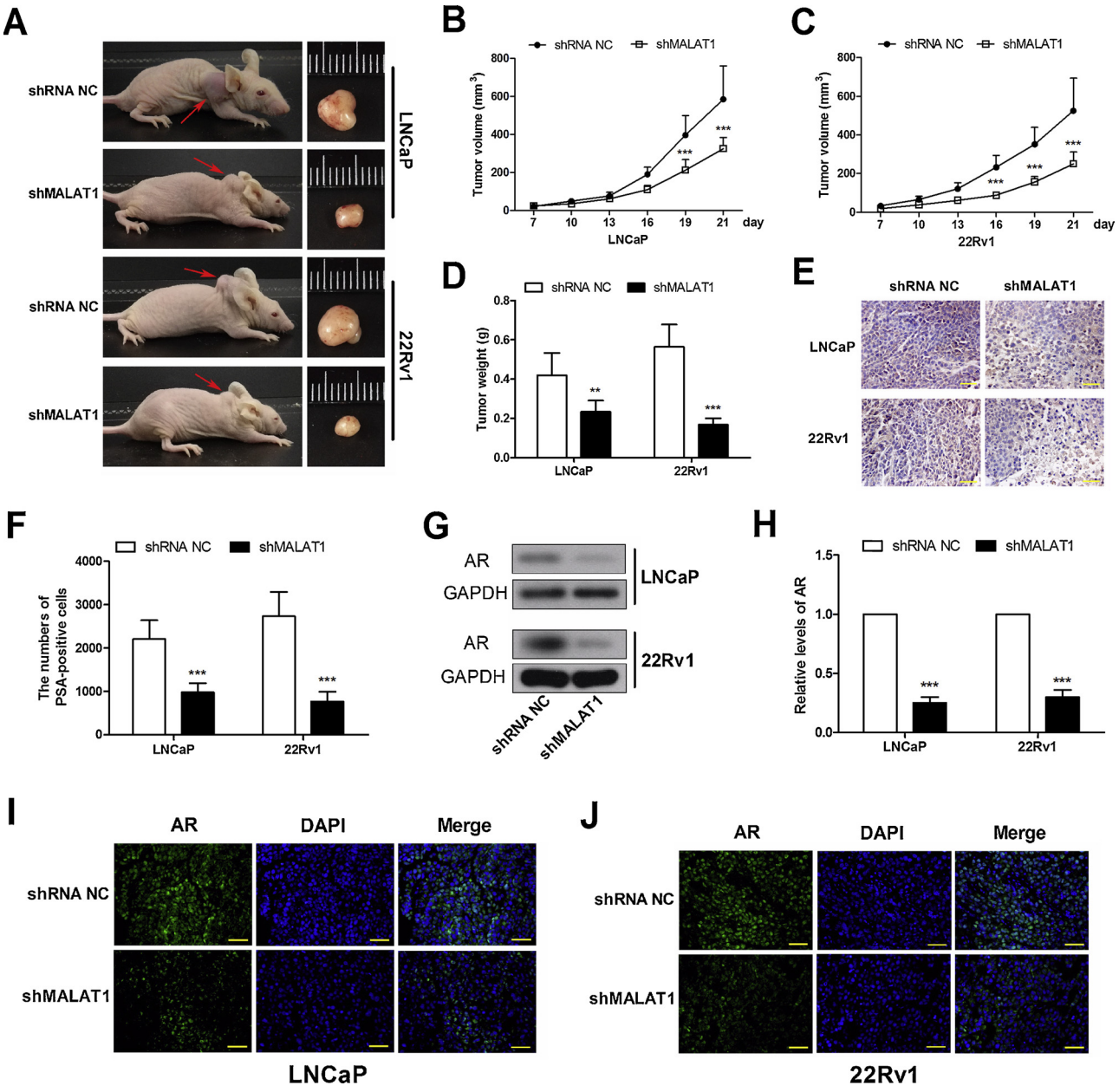

Fig. 6. MALAT1 knockdown inhibited tumorigenesis of prostate cancer cells *in vivo*.
(A) The nude representative mice inoculated with LNCaP or 22Rv1 cells with or without MALAT1 knockdown (the tumors were indicated with arrows) and the tumors isolated from the nude mice in each group. (B–C) The volume of subcutaneous tumors formed by LNCaP or 22Rv1 cells with or without MALAT1 knockdown at 7, 10, 13, 16, 19 or 21 day post inoculation. (D) The weight of tumors formed by LNCaP or 22Rv1 cells with or without MALAT1 knockdown at the 21st day after inoculation. (E) The immunohistochemical assay was performed to detect the PSA expression in tumors formed by LNCaP or 22Rv1 cells. (F) The numbers of PSA-positive cells in (E). (G–H) The AR expression levels in the tumors formed by LNCaP or 22Rv1 cells. (I–J) The immunofluorescence assay was performed to detect the expression of AR in tumors (H). (n = 6) (*$P < 0.05$, **$P < 0.01$, ***$P < 0.001$, *ns, no significance*; MALAT1, metastasis associated lung adenocarcinoma transcript 1, PSA, prostate specific antigen, AR, androgen receptor).

cancer and uterine endometrial stroma sarcoma [18–20], and the silencing of MALAT1 inhibits the malignancies of bladder cancer cells, cervical cancer cells [21,22]. It has also been reported that MALAT1 is highly expressed in prostate cancer specimens, and the knockdown of MALAT1 suppressed the proliferation, cell cycle progression, migration, invasion and tumorigenesis *in vivo* of prostate cancer cells [12]. Prostate cancer is an androgen-dependent tumor, however, the role of MALAT1 in prostate cancer cells under androgen or its analogue treatments has not been illustrated. As presented in Fig. S1, the DHT administration caused significant elevation of MALAT1 in AR-positive prostate cancer cells LNCaP and 22Rv1, which was much prominent than that in AR-negative cells DU145 and PC3 [23]. Thereby, these two androgen-sensitive prostate cancer cell lines, LNCaP and 22Rv1, were used subsequent experiments. After DHT treatment, the cell cycle transition from G1 to S phase of LNCaP and 22Rv1 cells was enhanced. At the same time, the MALAT1 and AR levels were increased upon DHT stimulation. In the MALAT1-silenced cells, the DHT-induced acceleration of cell cycle transition and increase of AR expression level were attenuated, suggested that MALAT1 may play its roles via AR signaling.

It is well-known that androgen and AR signaling play crucial roles in prostatic development, as well as prostate cancer progression. Although ADT is partly effective for prostate cancer, most patients develop into CRPC [3]. It has been reported that AR signaling is activated in CRPC, although ADT treatment leads to the low androgen level [24].

Numerous molecular alterations mediating AR signaling at low or absent androgen levels have been described in CRPC. AR overexpression is well-recognized in CRPC, and it can promote cell proliferation at low androgen levels [25]. Several studies have demonstrated that peptide molecules may transactivate the AR in the absence of ligand, including insulin like growth factors (IGF-I/II), epidermal growth factor (EGF), keratinocyte growth factor (KGF), and cytokines such as interleukin 6 (IL-6) [26]. The inhibition of IGF-IR was shown to affect AR translocation and transactivation *in vivo* [27]. Additionally, a number of AR co-activators are increased in CRPC including TIF-1, MAGE-II, SRB-1 and NFκB. Altered co-regulator expression may sensitize the AR for activation under low androgen conditions [28]. As the functions of AR signaling, numerous agents targeting AR have been developed, including AR antagonists, steroidogenic enzyme inhibitors, and other molecules that effect the transcription, translation, stability, localization and activity of AR [24]. AR is also regulated by miRNAs, such as miR-130a, miR-203 and miR-205 [29]. AR was targeted by miR-320 family, and downregulated by miR-320a [16]. MiR-320 family members share a same seed sequence. Our experiments demonstrated that miR-320b bound to AR and inhibited its expression. MiR-320b is downregualted in prostate cancer specimens, and inhibits proliferation by inactivating Wnt/β-catenin pathway in prostate cancer cells [30]. In our study, the expression level of miR-320b was decreased by DHT stimulation, which was opposite with that of MALAT1 and AR. The luciferase assay demonstrated that MALAT1 bound to miR-320b, regulated its expression, and vice versa, which suggested that MALAT1 may be a degradable sponge. The luciferase assay also showed the binding and regulation of miR-320b to AR. The phenotypic changes induced by shMALAT1 were abolished by transfection of miR-320b inhibitor or AR overexpresion plasmid, indicating that MALAT1 regulated AR signaling by sponging miR-320b, thereby control proliferation and cell cycle progression in prostate cancer cells.

LncRNAs play roles in multiple ways, wherein endogenous miRNA sponge hypothesis is most well-known [31]. MALAT1 has been reported to bind to miRNAs as a miRNA sponge or a competitive endogenous RNA. In our study, MALAT1 bound to miR-320b and negatively regulated its expression. Surprisingly, miR-320b also decreased the expression of MALAT1. So we hypothesized that MALAT1 is a degradable miRNA sponge [32].

5. Conclusion

In this study, we demonstrated that lncRNA MALAT1 was upregulated in prostate cancer cells after androgen stimulation, as well as AR. The silencing of MALAT1 inactivated AR signaling by sponging miR-320b, and inhibited proliferation and cell cycle progression in prostate cancer cells whether with androgen treatment or not. These findings suggested that MALAT1 may be a new target for diagnosis and therapy of prostate cancer in clinic.

Conflict of interest

The authors declare that they have no conflict of interest.

Appendix A. Supplementary data

Supplementary data associated with this article can be found, in the online version, at https://doi.org/10.1016/j.prp.2019.01.011.

References

[1] A. Jemal, F. Bray, M.M. Center, J. Ferlay, E. Ward, D. Forman, Global cancer statistics, CA Cancer J. Clin. 61 (2011) 69–90.

[2] G. Attard, C. Parker, R.A. Eeles, F. Schroder, S.A. Tomlins, I. Tannock, C.G. Drake, J.S. de Bono, Prostate cancer, Lancet 387 (2016) 70–82.

[3] X. Yuan, C. Cai, S. Chen, S. Chen, Z. Yu, S.P. Balk, Androgen receptor functions in castration-resistant prostate cancer and mechanisms of resistance to new agents targeting the androgen axis, Oncogene 33 (2014) 2815–2825.

[4] M. Huarte, The emerging role of lncRNAs in cancer, Nat. Med. 21 (2015) 1253–1261.

[5] A. Zhang, J. Zhang, A. Kaipainen, J.M. Lucas, H. Yang, Long non-coding RNA: a newly deciphered "code" in prostate cancer, Cancer Lett. 375 (2016) 323–330.

[6] C.A. Brosnan, O. Voinnet, The long and the short of noncoding RNAs, Curr. Opin. Cell Biol. 21 (2009) 416–425.

[7] R.A. Flynn, H.Y. Chang, Long noncoding RNAs in cell-fate programming and reprogramming, Cell Stem Cell 14 (2014) 752–761.

[8] P.J. Batista, H.Y. Chang, Long noncoding RNAs: cellular address codes in development and disease, Cell 152 (2013) 1298–1307.

[9] A.M. Schmitt, H.Y. Chang, Long noncoding RNAs in Cancer pathways, Cancer Cell 29 (2016) 452–463.

[10] M.J. Bussemakers, A. van Bokhoven, G.W. Verhaegh, F.P. Smit, H.F. Karthaus, J.A. Schalken, F.M. Debruyne, N. Ru, W.B. Isaacs, DD3: a new prostate-specific gene, highly overexpressed in prostate cancer, Cancer Res. 59 (1999) 5975–5979.

[11] J.R. Prensner, W. Chen, S. Han, M.K. Iyer, Q. Cao, V. Kothari, J.R. Evans, K.E. Knudsen, M.T. Paulsen, M. Ljungman, T.S. Lawrence, A.M. Chinnaiyan, F.Y. Feng, The long non-coding RNA PCAT-1 promotes prostate cancer cell proliferation through cMyc, Neoplasia 16 (2014) 900–908.

[12] S. Ren, Y. Liu, W. Xu, Y. Sun, J. Lu, F. Wang, M. Wei, J. Shen, J. Hou, X. Gao, C. Xu, J. Huang, Y. Zhao, Y. Sun, Long noncoding RNA MALAT-1 is a new potential therapeutic target for castration resistant prostate cancer, J. Urol. 190 (2013) 2278–2287.

[13] R. Wang, Y. Sun, L. Li, Y. Niu, W. Lin, C. Lin, E.S. Antonarakis, J. Luo, S. Yeh, C. Chang, Preclinical study using Malat1 small interfering RNA or androgen receptor splicing variant 7 degradation enhancer ASC-J9((R)) to suppress enzalutamide-resistant prostate Cancer progression, Eur. Urol. 72 (2017) 835–844.

[14] M.O. Ripple, W.F. Henry, R.P. Rago, G. Wilding, Prooxidant-antioxidant shift induced by androgen treatment of human prostate carcinoma cells, J. Natl. Cancer Inst. 89 (1997) 40–48.

[15] N. Craft, Y. Shostak, M. Carey, C.L. Sawyers, A mechanism for hormone-independent prostate cancer through modulation of androgen receptor signaling by the HER-2/neu tyrosine kinase, Nat. Med. 5 (1999) 280–285.

[16] S. Sato, K. Katsushima, K. Shinjo, A. Hatanaka, F. Ohka, S. Suzuki, A. Naiki-Ito, N. Soga, S. Takahashi, Y. Kondo, Histone deacetylase inhibition in prostate Cancer Triggers miR-320-Mediated suppression of the androgen receptor, Cancer Res. 76 (2016) 4192–4204.

[17] P. Ji, S. Diederichs, W. Wang, S. Boing, R. Metzger, P.M. Schneider, N. Tidow, B. Brandt, H. Buerger, E. Bulk, M. Thomas, W.E. Berdel, H. Serve, C. Muller-Tidow, MALAT-1, a novel noncoding RNA, and thymosin beta4 predict metastasis and survival in early-stage non-small cell lung cancer, Oncogene 22 (2003) 8031–8041.

[18] J.H. Luo, B. Ren, S. Keryanov, G.C. Tseng, U.N. Rao, S.P. Monga, S. Strom, A.J. Demetris, M. Nalesnik, Y.P. Yu, S. Ranganathan, G.K. Michalopoulos, Transcriptomic and genomic analysis of human hepatocellular carcinomas and hepatoblastomas, Hepatology 44 (2006) 1012–1024.

[19] A. Guffanti, M. Iacono, P. Pelucchi, N. Kim, G. Solda, L.J. Croft, R.J. Taft, E. Rizzi, M. Askarian-Amiri, R.J. Bonnal, M. Callari, F. Mignone, G. Pesole, G. Bertalot, L.R. Bernardi, A. Albertini, C. Lee, J.S. Mattick, I. Zucchi, G. De Bellis, A transcriptional sketch of a primary human breast cancer by 454 deep sequencing, BMC Genomics 10 (2009) 163.

[20] K. Yamada, J. Kano, H. Tsunoda, H. Yoshikawa, C. Okubo, T. Ishiyama, M. Noguchi, Phenotypic characterization of endometrial stromal sarcoma of the uterus, Cancer Sci. 97 (2006) 106–112.

[21] Y. Han, Y. Liu, L. Nie, Y. Gui, Z. Cai, Inducing cell proliferation inhibition, apoptosis, and motility reduction by silencing long noncoding ribonucleic acid metastasis-associated lung adenocarcinoma transcript 1 in urothelial carcinoma of the bladder, Urology 81 (209) (2013) e201–207.

[22] F. Guo, Y. Li, Y. Liu, J. Wang, Y. Li, G. Li, Inhibition of metastasis-associated lung adenocarcinoma transcript 1 in CaSki human cervical cancer cells suppresses cell proliferation and invasion, Acta Biochim Biophys Sin (Shanghai) 42 (2010) 224–229.

[23] A. van Bokhoven, M. Varella-Garcia, C. Korch, W.U. Johannes, E.E. Smith, H.L. Miller, S.K. Nordeen, G.J. Miller, M.S. Lucia, Molecular characterization of human prostate carcinoma cell lines, Prostate 57 (2003) 205–225.

[24] E.A. Mostaghel, S. Plymate, New hormonal therapies for castration-resistant prostate cancer, Endocrinol. Metab. Clin. North Am. 40 (2011) 625–642 x..

[25] C.D. Chen, D.S. Welsbie, C. Tran, S.H. Baek, R. Chen, R. Vessella, M.G. Rosenfeld, C.L. Sawyers, Molecular determinants of resistance to antiandrogen therapy, Nat. Med. 10 (2004) 33–39.

[26] Z. Culig, Androgen receptor cross-talk with cell signalling pathways, Growth Factors 22 (2004) 179–184.

[27] J.D. Wu, K. Haugk, L. Woodke, P. Nelson, I. Coleman, S.R. Plymate, Interaction of IGF signaling and the androgen receptor in prostate cancer progression, J. Cell. Biochem. 99 (2006) 392–401.

[28] P. Zhu, S.H. Baek, E.M. Bourk, K.A. Ohgi, I. Garcia-Bassets, H. Sanjo, S. Akira, P.F. Kotol, C.K. Glass, M.G. Rosenfeld, D.W. Rose, Macrophage/cancer cell interactions mediate hormone resistance by a nuclear receptor derepression pathway, Cell 124 (2006) 615–629.

[29] K. Boll, K. Reiche, K. Kasack, N. Morbt, A.K. Kretzschmar, J.M. Tomm, G. Verhaegh, J. Schalken, M. von Bergen, F. Horn, J. Hackermuller, MiR-130a, miR-203 and miR-205 jointly repress key oncogenic pathways and are downregulated in prostate carcinoma, Oncogene 32 (2013) 277–285.

[30] I.S. Hsieh, K.C. Chang, Y.T. Tsai, J.Y. Ke, P.J. Lu, K.H. Lee, S.D. Yeh, T.M. Hong, Y.L. Chen, MicroRNA-320 suppresses the stem cell-like characteristics of prostate cancer cells by downregulating the Wnt/beta-catenin signaling pathway, Carcinogenesis 34 (2013) 530–538.

[31] D.W. Thomson, M.E. Dinger, Endogenous microRNA sponges: evidence and controversy, Nat. Rev. Genet. 17 (2016) 272–283.

[32] Y. Yan, Q. Fan, L. Wang, Y. Zhou, J. Li, K. Zhou, LncRNA Snhg1, a non-degradable sponge for miR-338, promotes expression of proto-oncogene CST3 in primary esophageal cancer cells, Oncotarget 8 (2017) 35750–35760.